2.2

MEAN RADIANT TEMPERATURE MODELING OUTDOORS: A COMPARISON OF THREE APPROACHES

Csilla V Gál*[1] and Kerry A. Nice[2]
[1] Dalarna University, Falun, Sweden
[2] Monash University, Clayton, Australia

1 INTRODUCTION

The thermal environment of cities is deteriorating steadily owing to both urbanization and climate change. As a consequence, urban planners and city officials are increasingly under pressure to maintain livable urban environments. In this respect, numerical models offer the quickest and most economic means to assessing the performance and viability of various urban heat mitigation strategies. Owing to these advantages, the numerical approach gained popularity over the past decade—as indicated by the profusion of such studies and the proliferation of microclimate models.

The driving parameter of outdoor human thermal comfort is radiation, which is considered via the mean radiant temperature (T_{mrt}). This parameter expresses the short- and longwave radiation exchange of the human body in Celsius degrees. Here, the Celsius degree refers to the uniform temperature of an imaginary enclosure that results in an equivalent radiant heat exchange with the human body as the actual, non-uniform enclosure. Although T_{mrt} is at the center of most outdoor thermal comfort indices, it is both challenging to measure and to calculate. Together with the emergence of new microclimate models, the ways of calculating outdoor T_{mrt} have also grew in numbers. However, few studies have attempted to conduct a model intercomparison and to assess the impact of different T_{mrt} calculation methods. Therefore, the aim of this research is to assess the performance of three microclimate models in estimating T_{mrt} in the complex urban environments. The evaluated models are ENVI-met v4.4.2 (Bruse 1999) utilizing the Indexed View Sphere (IVS) algorithm, the Microclimate Map Analysis (Mackey 2015) component of Grasshopper and VTUF-3D v2 (Nice 2016).

2 MATERIALS AND METHODS

2.1 Study area and field measurement

The reference T_{mrt} values utilized in this study are derived from a 26-hour-long field experiment conducted at Bartók Square, Szeged (Hungary). The square, which measures 110 m x 55 m in size, is located in the downtown the city. The area is categorized as compact mid-rise (LCZ 2) according to the local climate zones classification scheme (Lelovics et al. 2014). The square is bounded by roads and by the continuous facades of 3–4 story buildings.

The field experiment was conducted during anti-cyclonic conditions over the late summer of 2016. The measurement started at 18:00 LST (one hour prior to sunset) on the 7th of August and concluded at 20:00 LST (one hour after sunset) on the following day. During the time of the measurement, the air temperature in the city remained within the 17.1–26.9 °C range and global radiation peaked at 848 W m^{-2} according to the urban weather station of Szeged (Fig. 1).

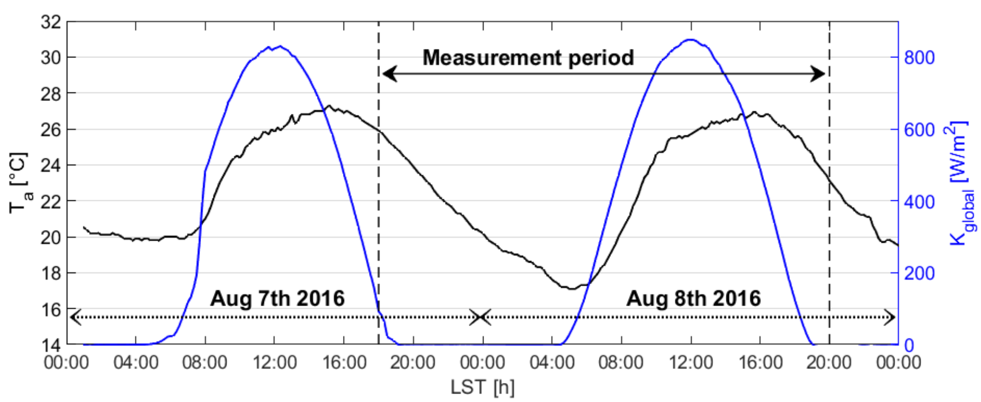

Figure 1. The development of global horizontal radiation (blue) and air temperature (black) in the city during August 7th and 8th 2016 according to the urban weather station of Szeged

* *Corresponding author address*: Csilla V. Gál, Dalarna University, Falun 79188, Sweden; e-mail: cga@du.se

The measurement utilized a human-biometeorological station and recorded radiation data along the four facades of the square—at sites P1–P4 (Fig. 2). Short- and longwave radiation data were collected according Höppe's (1992) six-directional method. A full account of the measurement is reported in Kántor et al. (2018).

2.2 The microclimate models and their assessment

ENVI-met is a prognostic, three-dimensional, high-resolution microclimate model designed to simulate surface-plant-air interactions at the micro- to local scales. It is a non-hydrostatic, obstacle-resolving computational fluid dynamics (CFD) model that relies on Reynolds Averaged Navier-Stokes (RANS) equations. The model has been initially developed by Bruse as part of his dissertation (1999). The Indexed View Sphere (IVS) algorithm— which retains the view factor-element connection in the calculation of radiation fluxes in the domain—was introduced with v4.1.1. T_{mrt} calculation in ENVI-met is based on the German VDI Standard (*Verein Deutscher Ingenieure,* 1998, 2001), which have adopted the approach of Fanger (1972) and that of Jendritzky and Nübler (1981). In the absence of direct solar radiation, the approach derives T_{mrt} as the sum of human-absorbed diffuse radiation components (both short- and longwave). When direct solar radiation is present, the formula is complemented with a term after Jendritzky et al. (1990). It divides the three-dimensional space into upper and lower hemispheres and assumes that 50% of the radiation will arrive from the sky and 50% from the ground (Huttner 2012; Ali-Toudert 2005). In the calculation of the absorbed direct shortwave radiation component, ENVI-met relies on the Underwood and Ward's (1966) projected area factor formula. This formula is derived for an elliptical cylinder model with its major axis facing the sun.

The Microclimate Map Analysis (Mackey 2015) is a Honeybee component, which is one of Grasshopper's many plugins. The Microclimate Map Analysis is able to calculate outdoor thermal comfort utilizing EnergyPlus-derived surface temperatures. It's T_{mrt} calculation method is based on the effective radiant field (ERF) approach of Arens et al. (1986, 2014). In concept, the ERF approach is similar to that utilized in ENVI-met. It begins with the calculation of absorbed diffuse long- and shortwave radiation fluxes (that is the so called base T_{mrt}). The resultant value is then complemented with the absorbed direct solar radiation component. Microclimate Map Analysis assumes a seated subject and utilizes the projected area factors derived by Fanger (1972).

VTUF-3D (Vegetated Temperatures of Urban Facets) is a micro-scale energy balance model developed by Nice (2016) as part of his dissertation. The model integrated MAESPA, a forest canopy radiation absorption, photosynthesis and water balance model of Duursma and Medlyn (2012), into TUF-3D—the urban micro-climate surface energy balance model of Krayenhoff and Voogt (2007). VTUF-3D is able to simulate the vegetation-radiation interaction in complex urban environments. The model adopted a two-step approach to calculating T_{mrt}. First, it derives 'virtual' globe temperature (T_g) values by solving the energy balance equation of Liljegren et al. (2008). Then, it calculates T_{mrt} from the thus obtained T_g values with the help of the formula published in Kántor and Unger (2011). The different parameters adopted by the models in reference to the human subject are summarized in Table 1

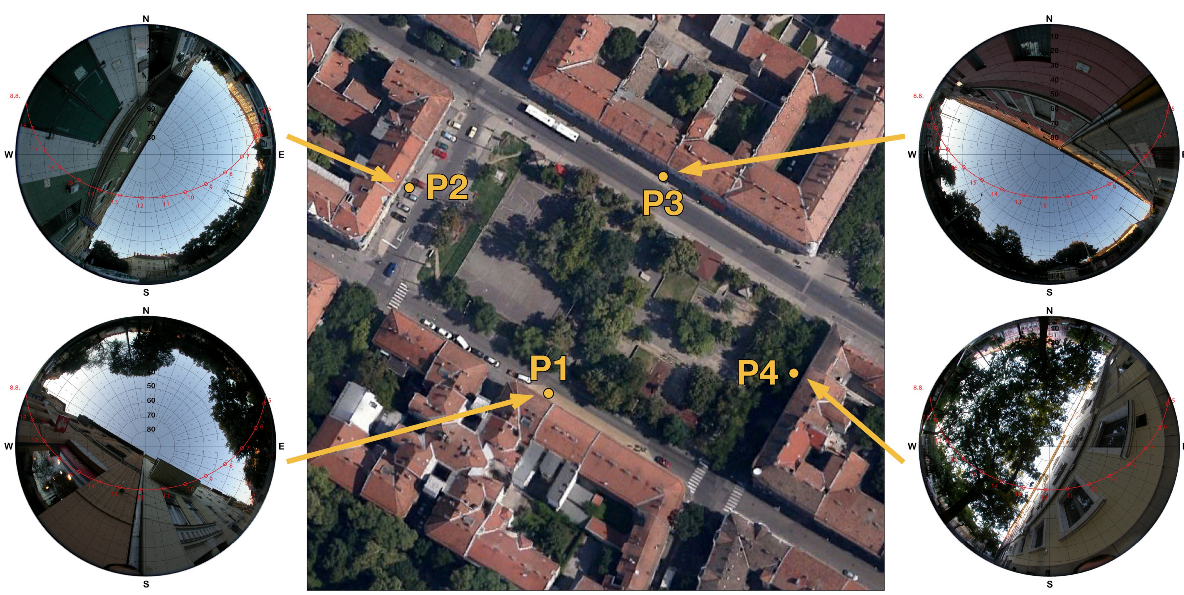

Figure 2. The four measurement sites at Bartók Square and the corresponding fisheye images.

Table 1. Human parameters adopted by the models

Numerical models	***SW rad. absorpt.***	***LW rad. absorpt.***	***Posture***
ENVI-met	0.70	0.97	standing
Microclimate Map Analysis	0.70	0.95	seated
VTUF-3D	T_g	T_g	squatting

The domains representing Bartók Square and its surrounding are developed with the use of (a) the available GIS and digital elevation maps, (b) the urban tree inventory of the city (Kiss et al. 2015; Takács et al. 2015), and (c) Google Earth aerial imagery and additional onsite surveys. Since the square has a nearly flat terrain with ground elevation differences largely remaining below 0.5 m, the square is modeled as flat in all three domains. The spatial resolution of the domains is shown in Table 2. In the case of the Microclimate Map Analysis, surface temperatures are calculated at 6 m x 6 m resolution, while the absorbed radiation fluxes are calculated on the basis of sky view factors derived from a finer 3 m x 3 m domain resolution. The albedo and emissivity values of urban surfaces and obstacles is set uniformly across all three models. The adopted values are summarized in Table 3.

Table 2. Horizontal spatial resolution of the domains

Numerical models	**Domain grid size**
ENVI-met	3 x 3 m
Microclimate Map Analysis	6 m x 6 m (T_s) 3 m x 3 m
VTUF-3D	5 m x 5 m

Table 3. Surface properties and their values used with obstacles and the ground in the domains

Obstacles and surfaces	**Albedo**	**Emissivity**	**Transmis-sivity**
Ground	0.18	0.95	-
Wall	0.20	0.90	-
Tree	0.20	0.95-0.96	0.07

The meteorological data used to force the models is obtained from the urban weather station of Szeged. The weather station is operated by the Hungarian Meteorological Service and located 900 m from the square. All numerical simulations were run for a 48-hour period with the start date set at August 7th, 2018 00:00 LST. Model states are saved at 15-minute intervals, except for the Microclimate Map Analysis Grasshopper component. The latter model had an hourly temporal resolution and the results were interpolated to adequate times to match the time of observations (i.e. values from P2 are interpolated to the 15th minute of every hour, values from P3 to the 30th minute of every hour, while values from P4 to the 45th minute of every hour). The interpolation followed a standard procedure adopted also by the EnergyPlus software (see National Renewable Energy Laboratory n.d.).

The performance of models to reproduce T_{mrt} values is evaluated on a single point basis. In order to reduce errors, location sensitivity analyses were conduced for each model and site. Data from domain cells with the best fit are used in the analysis. The performances assessment of the models relies both on linear regression parameters and difference measures (Willmott 1981, 1982). The statistical parameters reported are: the number of observations (n), the mean absolute error (MAE), the root mean square error (RMSE), the systematic root mean square error ($RMSE_S$), the unsystematic root mean square error ($RMSE_u$), the index of agreement (d) and the coefficient of determination (R^2). All data-processing is performed in MATLAB.

3 RESULTS

The scatter plots of observed-modeled T_{mrt} values and the respective linear regression lines per models is presented in Fig. 3. The data pairs are differentiated by the shading condition that prevailed during the observation: (o) refers to sunlit, (x) to shaded and (.) to nighttime conditions. According to the results, ENVI-met systematically underestimates T_{mrt} over the day. Microclimate Map Analysis reproduces nighttime T_{mrt} values well, but the mid-range daytime values exhibit a greater scatter. VTUF-3D slightly underestimates nighttime T_{mrt}. Its magnitude of errors increases with increasing T_{mrt} values.

The statistical parameters depicting the ability of the models to reproduce T_{mrt} are presented in Table 4. According to the the index of agreement values (d) all three models are relatively error free: ENVI-met (95%) Microclimate Map Analysis (96%), and VTUF-3D (92%). The index of determination (R^2) values vary at a wider range. Accordingly, ENVI-met is able to reproduce 96%, Microclimate Map Analysis 87% and VTUF-3D 77% variance in the data. Based on the index of agreement values ENVI-met (0.95) and the Microclimate Map Analysis (0.96) are able to estimate the observed T_{mrt} trends well. In terms of total model errors (RMSE), the Microclimate Map Analysis performs better than ENVI-met (the respective values are 6.20 ºC and 7.11 ºC). However, ENVI-met has the lowest unsystematic errors ($RMSE_u$ = 3.21 ºC), which indicates a strong potential for accuracy once the linear biases in the models are reduced. The weakest model of the three is VTUF-3D. It has the highest RMSE (9.05 ºC) and $RMSE_u$ (8.51 ºC) values with the lowest index of agreement (0.92).

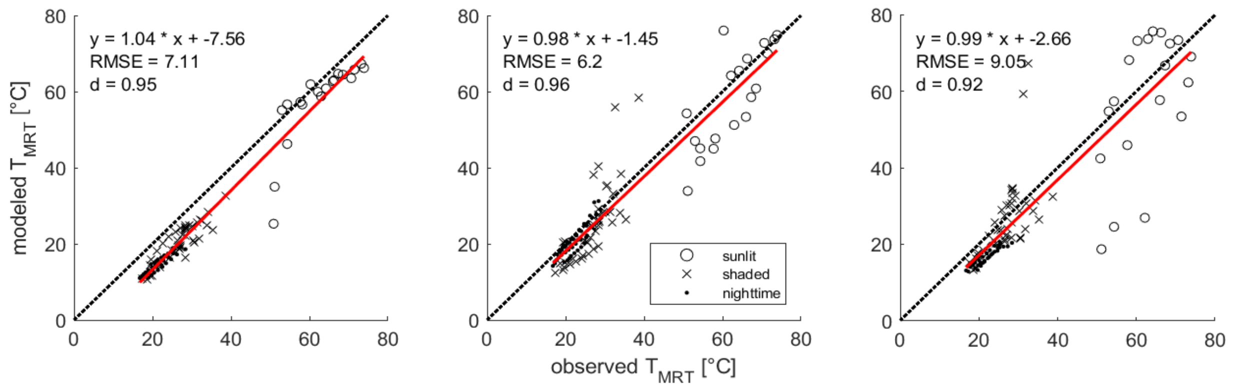

Figure 3. Scatterplots of observed-modeled T_{mrt} values: ENVI-met (left), Microclimate Map Analysis (center), and VTUF-3D (right).

Table 4. Statistical evaluation of the models' ability to reproduce observed T_{mrt} values

	n	ME	MAE	RMSE	$RMSE_s$	$RMSE_u$	d	R^2
ENVI-met	104	-6.32	6.43	7.11	6.35	3.21	0.95	0.96
Microclimate Map Analysis	104	-2.13	4.43	6.2	2.16	5.82	0.96	0.87
VTUF-3d	104	-3.05	6.35	9.05	3.06	8.51	0.92	0.77

Fig. 4 presents the diurnal course of measured (black) and modeled (blue) T_{mrt} values across models for the relatively shaded sites: P1 (left column) and P4 (right column). The three images within the columns refer to the results obtained from ENVI-met (top), Microclimate Map Analysis (middle) and VTUF-3D (bottom) respectively. The times of sunrise/sunset at these images are signaled by vertical dashed lines. The vertical dotted lines refer to the times when a given site moves in or our of shade. A general comparison of observed and modeled T_{mrt} values indicate that all models are able to reproduce the diurnal trends well. The greatest errors occur during the time the sites moves in or out of shade. This is especially true at site P4 under the tree (see images in the right column). After 13:00 LST, this site becomes briefly irradiated by the sun through the overlying tree canopy. This event hard to reproduce with numerical models partly because of their spatial resolution—see for example the results of VTUF-3D with the largest domain resolution. The simplified way tree canopies are defined in these models also explains these errors.

At night, the models generally underestimate T_{mrt}. The systematic underestimation ranges from about 2-5 ºC in the case of Microclimate Map Analysis (Fig. 4., middle row of images) to about 6-8 ºC in the case of ENVI-met (see Fig. 4., top row of images). ENVI-met's systematic underestimation of T_{mrt} continues during the day when the sites are in shade—albeit with a lesser magnitude. The results of Microclimate Map Analysis indicate issues with estimating radiation fluxes under the tree (Fig. 4., right column, middle image). In fact, among the evaluated models, the treatment of trees is the most rudimentary in this model. VTUF-3D is able to reproduce T_{mrt} under the tree well. However, at the site P1 with northerly exposure, VTUF-3D overestimates afternoon T_{mrt} values in shade by up to 6 ºC (Fig. 4., left column, bottom image). In the morning, site P1 became sunlit for about two hours. Except for Microclimate Map Analysis, the models were able to reproduce sunlit T_{mrt} values well.

Fig. 5 presents the diurnal course of measured (black) and modeled (blue) T_{mrt} values across models at the predominantly sunlit sites: P2 (left column) and P3 (right column). Similarly, to Fig. 4, the three images within the columns refer to the results obtained from the three models: ENVI-met (top), Microclimate Map Analysis (middle) and VTUF-3D (bottom). However, in the case of ENVI-met the original results (blue) are supplemented with recalculated (red) T_{mrt} values. In the recalculation, the ENVI-met adopted *Underwood and Ward* (1966) projected area factor formula was replaced with that of Jendritzky et al. (1990). The latter projected area factor formula is also adopted by RayMan (Matzarakis et al. 2010) and the German VDI Standard (Verein Deutscher Ingenieure 1998, 2001). In Fig. 5, the times of sunrise/sunset and the times a site moves in or out of shade are likewise indicated by vertical dashed and dotted lines, respectively.

At the sites with prolonged direct solar radiation, Microclimate Map Analysis estimates nighttime T_{mrt} values the best with insignificant errors (Fig. 5, middle row). In contrast, the systematic underestimation of T_{mrt} by ENVI-met during the same period is 8-10 ºC. VTUF-3D also underestimates T_{mrt} values at night, although to a lesser extent (by about 5 and 8 ºC at site P3 and P4, respectively). Similarly to the relatively shaded sites (P1 and P4, Fig. 4), ENVI-met systematically under-estimates T_{mrt} values at the more exposed ones (P2 and P4, Fig. 5) when at sites are in shade. However, in the case of the latter, more exposed sites, the underestimation is significant (up to 10 ºC). VTUF-3D also underestimates T_{mrt} values by about 3—5 ºC at the P2 and P3 sites when they are in shade. This is in contrast to the mode's behavior at the more shaded sites (see Fig. 4). The performance of the Microclimate Map Analysis is mixed: it estimates T_{mrt} values well at site P2 (with some errors when the site becomes shaded) and underestimates them at site P3.

During the time of prolonged direct solar radiation, ENVI-met reproduces T_{mrt} values the best among the models. However, the T_{mrt} values recalculated using Jendritzky et al.'s (1990) projected area factor formula reveal that these values would be significantly underestimated (by up to about 10 and 15 ºC at P2 and P3 sites, respectively), if a more appropriate formula would have been adopted by the mode. During times of prolonged direct solar radiation, VTUF-3D both under- and overestimates T_{mrt}. The trend of this under- and overestimation follows the changes in solar altitude angles: underestimation occurs at low and overestimation at high sun angles. The trend of these errors are in agreement with the findings of Thorsson et al. (2007). The authors demonstrated that T_{mrt} values derived from globe temperature measurement (or for a sphere shape using the six-directional radiation method of Höppe) have a tendency to underestimate T_{mrt} at low sun angels when compared to T_{mrt} values calculated using the six-directional method for a standing man. Although the T_{mrt} estimates of Microclimate Map Analysis are also quite accurate at site P3 (Fig. 5, middle right image), at P2 sites the model significantly underestimates T_{mrt} values with a trend similar to that discussed in conjunction with VTUF-3D. This might be due to the fact that Microclimate Map Analysis assumes a sitting subject in its T_{mrt} calculation.

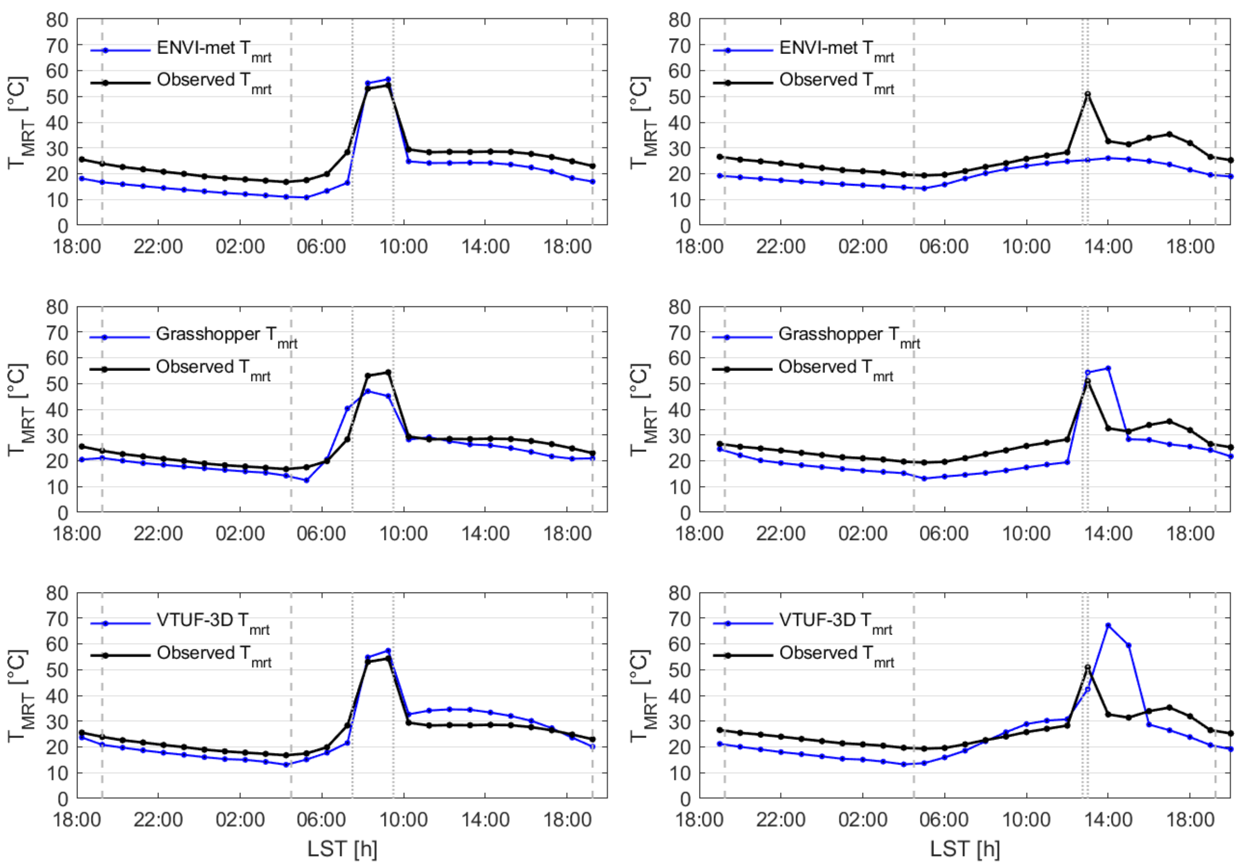

Figure 4. Diurnal course of T_{mrt} at the shaded sites: P1 (left column) and P4 (right column). The top row of images refer to results from ENVI-met, the middle ones are from Microclimate Map Analysis and the bottom ones from VTUF-3D.

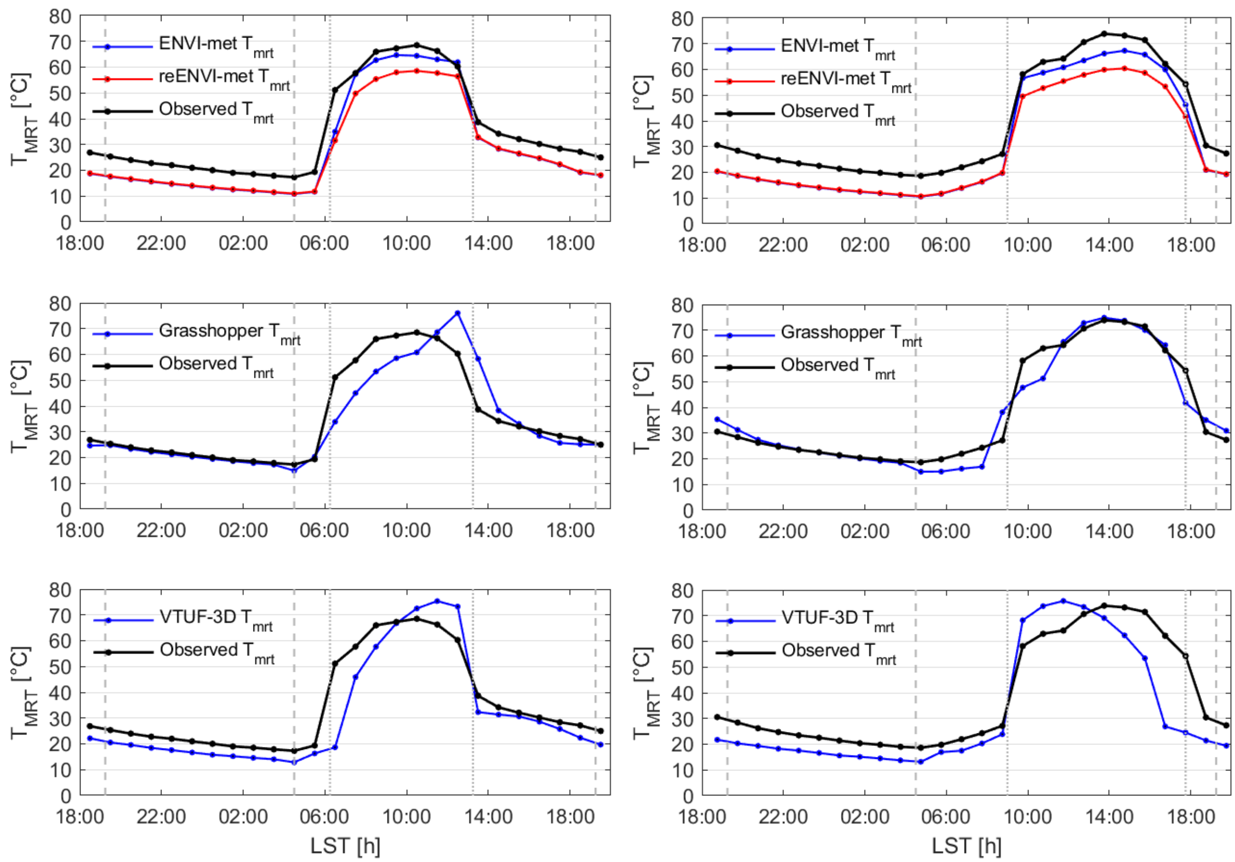

Figure 5. Diurnal course of T_{mrt} at the sunlit sites: P2 (left column) and P3 (right column). The top row of images refer to results from ENVI-met, the middle ones are from Microclimate Map Analysis and the bottom ones from VTUF-3D. In the case of ENVI-met, the results have been complemented with re-calculated T_{mrt} values (red) utilizing Fanger's projected area factor values (see text for further explanation).

4. DISCUSSION

As discussed in the previous section, considerable differences between the model estimated T_{mrt} values may occur as a result of differences in: (a) domain resolution, (b) the adopted projected area factor formula and (c) the assumed posture and/or calculation method. In order to reveal T_{mrt} differences owing to different calculation methods, the observation-derived T_{mrt} values were recalculated using the method of adopted by ENVI-met with the projected area factor formula of Jendritzky et al. (1990). First the sum of absorbed short- and longwave radiation fluxes (K^*_{obs} and L^*_{obs}, respectively) were calculated separately with Höppe's six directional approach. Then, the same components were derived utilizing the method of ENVI-met from measured up- and downwelling short- and longwave radiation fluxes. Since the latter method requires direct beam radiation values, the global solar radiation data obtained from the urban weather station was partitioned utilizing the formula of Reindl et al. (1990) and the horizontal component of the beam radiation was subtracted from the site-measured downwelling shortwave radiation values when the sites were sunlit.

The results are shown on Fig. 6. The top row presents to the shaded sites (P1, left side and P4 right side), and the bottom row the sites with prolong solar radiation exposure (P2, left side and P3, right side). The absorbed short- and longwave radiation components are both distinguished by colors and are plotted at the opposite side of the abscissa: the shortwave ones above the coordinate, with reddish hues and longwave ones below the coordinate with greenish hues. The symbols in the legend refer to the following radiation fluxes: absorbed direct solar radiation (K^*_{beam}), absorbed diffuse shortwave radiation from the upper hemisphere ($K^*_{sky+ref}$), absorbed shortwave radiation from the lower hemisphere (L^*_{UH}), absorbed longwave radiation from the upper hemisphere (L^*_{UH}), and absorbed longwave radiation from the lower hemisphere (L^*_{LH}). These components are plotted as stacked curves in order to allow for a direct comparison with the six-directional method derived K^*_{obs} and L^*_{obs} values (indicated by bold red and blue lines, respectively).

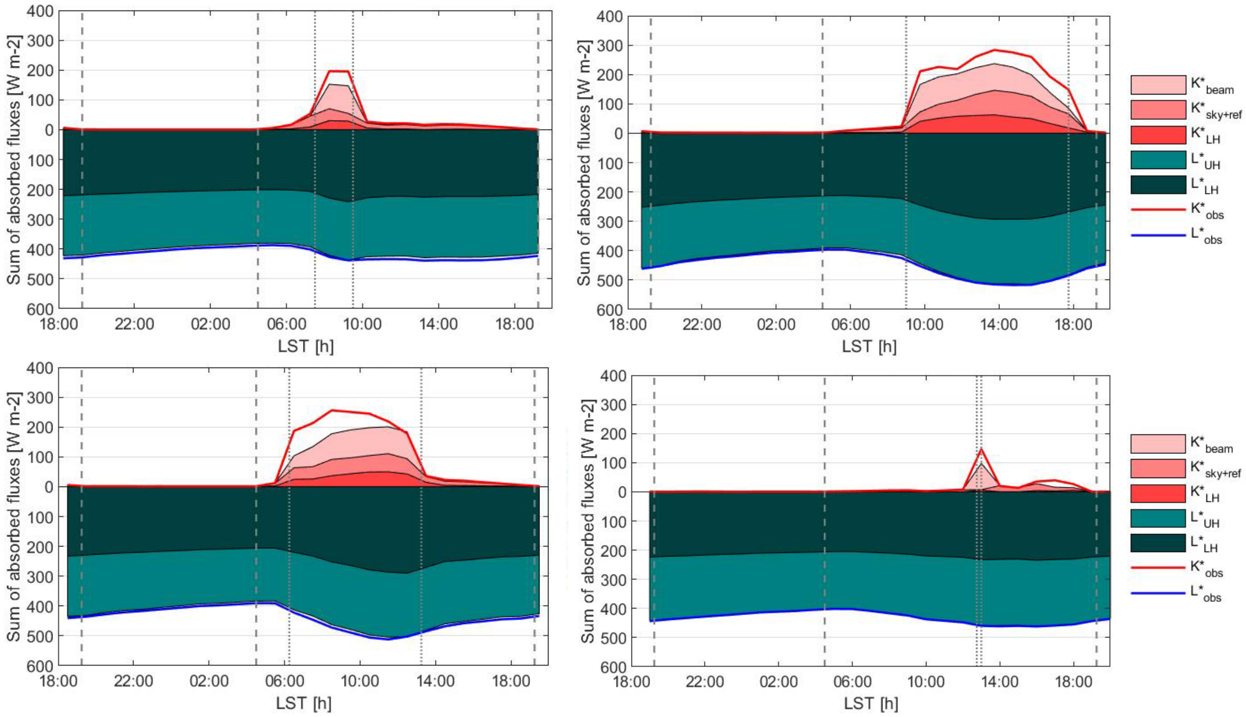

Figure 6. Diurnal course of absorbed short- and longwave radiation fluxes by a standing man, calculated from observed radiation fluxes utilizing the T_{mrt} calculation method of ENVI-met (see text for further explanation): P1 site (top left), P4 site (top right), P2 site (bottom left) and P3 site (bottom right).

As shown by Fig. 6, the difference between the two calculation method is characteristic to shortwave radiation fluxes and greatest during times of direct solar radiation exposure. The discrepancy between the two calculation methods was also highlighted Holmer et al. (2018). The authors pointed out that in the ENVI-met adopted T_{mrt} calculation approach the diffusely reflected and/or emitted short- and longwave radiation components account only for the origin of these fluxes in the three-dimensional space (via angle factors). Consequently, the approach renders the human body into a flat surface. The authors recommended the introduction of shape factors into the calculation of the absorbed diffuse radiation fluxes, as initially recommended by Höppe (1992) (Holmer et al. 2018).

5. CONCLUSIONS

The study assessed the ability of three human-biometeorological models to estimate T_{mrt} values in complex urban environments. The T_{mrt} estimates of the three models were compared both to those obtained via a 26-hour-long filed measurement utilizing Höppe's (1992) six-directional method and to each other (model intercomparison). According to the results, all models are able to reproduce the observed T_{mrt} trends well with index of agreement values between 0.92—0.96. Although the Microclimate Map Analysis has the lowest RMSE value (6.20 ºC), ENVI-met has the greatest potential for accuracy. The latter one is indicated by the model's $RMSE_u$ value, which is the lowest (3.21 ºC) among the examined models.

ENVI-met systematically underestimates T_{mrt} values at night and when the sites are in shade. Although Microclimate Map Analysis and VTUF-3D are able to reproduce nighttime T_{mrt} values better, they considerably underperform when the sites are exposed to extended periods of direct solar radiation. Some of the latter discrepancies are the result of different domain resolutions—as in the case of VTUF-3D with the greatest resolution. However, the assumed postures (sitting in the case of Microclimate Map Analysis) and the adopted calculation methods also play a significant role in these errors. In the case of VTUF-3D, T_{mrt} values are derived from virtual globe temperature (T_g) values, calculated after the formula of Liljegren et al. (2008). Consequently, during time of prolonged direct solar radiation, the pattern of errors corresponds to that observed when T_{mrt} is derived from measured T_g values. Furthermore, the T_{mrt} calculation method adopted by ENVI-met also carries inherent biases. However, since these errors are most pronounced when the sites are exposed to direct solar radiation, they are largely compensated by the projected area factor formula of the model. Compared to the projected area factor formula of Jendritzky et al. (1990), ENVI-met's approach increases the model-estimated T_{mrt} values by up to 8 ºC when the sites are sunlit.

REFERENCES

Ali-Toudert, F., 2005: Dependence of outdoor thermal comfort on street design in hot and dry climate. Doctoral dissertation, Meteorologisches Instituts der Albert-Ludwigs-Universität, urn:nbn:de:bsz:25-opus-20789

Arens, E., R. Gonzalez, and L. Berglund, 1986: Thermal comfort under an extended range of environmental conditions. *ASHRAE Trans.*, **92**, 18–26.

Arens, E., T. Hoyt, X. Zhou, L. Huang, H. Zhang, and S. Schiavon, 2015: Modeling the comfort effects of short-wave solar radiation indoors. *Build. Environ.*, **88**, 3–9, https://doi.org/10.1016/j.buildenv.2014.09.004

Bruse, M., 1999: Die Auswirkungen kleinskaliger Umweltgestaltung auf das Mikroklima [The impacts of small-scale environmental modifications on the microclimate]. Doctoral dissertation, Ruhr-Universität Bochum. https://doi.org/10.23689/fidgeo-440

Duursma, R. A., and B. E. Medlyn, 2012: MAESPA: A model to study interactions between water limitation, environmental drivers and vegetation function at tree and stand levels, with an example application to [CO2] × drought interactions. *Geosci. Model Dev.*, **5**, 919–940, https://doi.org/10.5194/gmd-5-919-2012

Fanger, P. O., 1972: *Thermal comfort: Analysis and applications in environmental engineering*. McGrew-Hill,.

Holmer, B., F. Lindberg, and S. Thorsson, 2018: Mean radiant temperature and the shape of the standing man. *10th International Conference on Urban Climate*, New York City, NY, https://ams.confex.com/ams/ICUC10/meetingapp.cgi/Paper/342581

Höppe, P., 1992: Ein neues Verfahren zur Bestimmung der mittleren Strahlungstemperatur im Freien [A new method to determine the mean radiation temperature outdoors]. *Wetter und Leb.*, **44**, 147–151.

Huttner, S., 2012: Further development and application of the 3D microclimate simulation ENVI-met. Doctoral dissertation, Johannes Gutenberg-Universität, 137 pp.

Jendritzky G., Menz G., Schmidt-Kessen W., S. H., 1990: *Methodik zur räumlichen Bewertung der thermischen Komponente im Bioklima des Menschen, Fortgeschriebenes Klima-Michel-Modell [Methodology for the spatial evaluation of the thermal component in the bioclimate of humans, Updated Klima-Michel model]*. Beiträge Nr. 114. Akademie für Raumforschung und Landesplanung, 80 pp.

Jendritzky, G., and W. Nübler, 1981: A model analysing the urban thermal environment in physiologically significant terms. *Arch. Meteorol. Geophys. Bioclimatol. Ser. B*, **29**, 313–326, https://doi.org/10.1007/BF02263308

Kántor, N., and J. Unger, 2011: The most problematic variable in the course of human-biometeorological comfort assessment - The mean radiant temperature. *Cent. Eur. J. Geosci.*, **3**, 90–100, https://doi.org/10.2478/s13533-011-0010-x

Kántor, N., C. V. Gál, Á. Gulyás, and J. Unger, 2018: The impact of façade orientation and woody vegetation on summertime heat stress patterns in a Central European square: comparison of radiation measurements and simulations. *Adv. Meteorol.*, **2018**, https://doi.org/10.1155/2018/2650642

Kiss, M., Á. Takács, R. Pogácsás, and Á. Gulyás, 2015: The role of ecosystem services in climate and air quality in urban areas: Evaluating carbon sequestration and air pollution removal by street and park trees in Szeged (Hungary). *Morav. Geogr. Reports*, **23**, 36–46, https://doi.org/10.1515/mgr-2015-0016

Krayenhoff, S. E., and J. A. Voogt, 2007: A microscale three-dimensional urban energy balance model for studying surface temperatures. *Boundary-Layer Meteorol.*, **123**, 433–461, https://doi.org/10.1007/s10546-006-9153-6

Lelovics, E., J. Unger, T. Gál, and C. V. Gál, 2014: Design of an urban monitoring network based on Local Climate Zone mapping and temperature pattern modelling. *Clim. Res.*, **60**, 51–62, https://doi.org/10.3354/cr01220

Liljegren, J. C., R. A. Carhart, P. Lawday, S. Tschopp, and R. Sharp, 2008: Modeling the wet bulb globe temperature using standard meteorological measurements. *J. Occup. Environ. Hyg.*, **5**, 645–655, https://doi.org/10.1080/15459620802310770

Mackey, C. W., 2015: Pan climatic humans: shaping thermal habits in an unconditioned society. M.S. thesis, Department of Architecture, Massachusetts Institute of Technology. https://dspace.mit.edu/handle/1721.1/99261

Matzarakis, A., F. Rutz, and H. Mayer, 2010: Modelling radiation fluxes in simple and complex environments: basics of the RayMan model. *Int. J. Biometeorol.*, **54**, 131–139, https://doi.org/10.1007/s00484-009-0261-0

National Renewable Energy Laboratory, n.d.: Weather data hourly interpolation. Accessed April 27, 2017, https://www.energyplus.net/sites/default/files/docs/site_v8.3.0/InputOutputReference/07-WeatherData/index.html#weather-data-hourly-interpolation

Nice, K., 2016: Development, validation, and demonstration of the VTUF-3D v1.0 urban micro-climate model to support assessments of urban vegetation influences on human thermal comfort. Doctoral dissertation, Monash University. https://doi.org/10.4225/03/58ace3cbb17bc

Reindl, D. T., W. A. Beckman, and J. A. Duffie, 1990: Diffuse fraction correlations. *Sol. Energy*, **45**, 1–7, https://doi.org/10.1016/0038-092X(90)90060-P

Takács, Á., M. Kiss, E. Tanács, L. Varga, and Á. Gulyás, 2015: Investigation of tree stands of public spaces in Szeged. *J. Environ. Geogr.*, **8**, 33–39, https://doi.org/10.1515/jengeo-2015-0010

Thorsson, S., F. Lindberg, I. Eliasson, and B. Holmer, 2007: Different methods for estimating the mean radiant temperature in an outdoor urban setting. *Int. J. Climatol.*, **27**, 1983–1993, https://doi.org/https://doi-org.www.bibproxy.du.se/10.1002/joc.1537

Underwood, C. R., and E. J. Ward, 1966: The solar radiation area of man. *Ergonomics*, **9**, 155–168, https://doi.org/10.1080/00140136608964361

Verein Deutscher Ingenieure, 1998: *Umweltmeteorologie: Methoden zur human-biometeorologischen Bewertung von Klima und Lufthygiene für die Stadt- und Regionalplanung, Teil 1: Klima [Environmental meteorology: methods for the human biometeorological evaluation of climate and air quality for urban and regional planning at regional level. Part 1: Climate] (VDI 3787, Part I)*. Beuth.

Verein Deutscher Ingenieure, 2001: *Umweltmeteorologie: Wechselwirkungen zwischen Atmosphäre und Oberflächen, Berechnung der spektralen Bestrahlungsstärken im solaren Wellenlängenbereich [Environmental Meteorology: Interactions between atmosphere and surfaces, calculation of spectral irradiances in the solar wavelength range] (VDI 3789, Part 3)*. Beuth.

Willmott, C. J., 1981: On the validation of models. *Phys. Geogr.*, **2**, 184–194.

Willmott, C. J., 1982: Some comments on the evaluation of model performance. *Bull. Amer. Meteor. Soc.*, **63**, 1309–1313.